Temin, H., & Baltimore, D. (1972) *Adv. Virus Res. 17*, 129.
Thomas, K. R., & Olivera, B. M. (1978) *J. Biol. Chem. 253*, 424.
Varmus, H. E., Heasley, S., Kung, H. J., Oppermann, H., Smith, V. C., Bishop, J. M., & Shank, P. R. (1978) *J. Mol. Biol. 120*, 55.
Verma, I. (1977) *Biochim. Biophys. Acta 473*, 1.
Verma, I. M. (1975) *J. Virol. 15*, 843.
Verma, I. M., & Baltimore, D. (1973) *Methods Enzymol. 29*, 125.
Watson, K. F., Schendel, P. L., Rosok, H. J., & Ramsey, L. R. (1979) *Biochemistry 18*, 3210.
Wu, A. M., & Gallo, R. C. (1976) *C.R.C. Crit. Rev. Biochem. 3*, 289.

Hydrogen-1 and Phosphorus-31 Nuclear Magnetic Resonance Study of the Solution Structure of *Bacillus licheniformis* 5S Ribonucleic Acid†

P. J. M. Salemink,* H. A. Raué,* A. Heerschap, R. J. Planta, and C. W. Hilbers*

ABSTRACT: The conformation of *Bacillus licheniformis* 5S RNA in solution has been studied by using 360-MHz ^{1}H NMR and 40.5-MHz ^{31}P NMR spectroscopy. The ^{1}H NMR spectra, which are well resolved, have been compared with theoretical spectra derived by ring current shift calculations for various models proposed in the literature for the secondary structure of 5S RNA. The total amount of base pairs is estimated to be around 36. NMR melting experiments indicate that both the molecular stalk and the prokaryotic loop [Fox, G. E., & Woese, C. R. (1975) *Nature (London) 256*, 505] are present in the solution structure. On this basis, some models proposed for the secondary structure of 5S RNA not containing these structural features can be rejected. Several resonances are observed around 10.7 ppm that can be ascribed to protons involved in non-Watson–Crick base pairing most likely present in tertiary interactions in the 5S RNA molecule or to ring N protons of nonpaired bases which as a result of the molecular folding are shielded from the solvent. Under our solution conditions, these structural features disappear at physiological temperature, the process being uncoupled from the collapse of the secondary structure. Using ^{31}P NMR, we demonstrate that the number of phosphate conformations in the sugar phosphate backbone of 5S RNA, deviating from the g^-,g^- conformation normally found in double helices, is far less than in tRNA.

5S RNA is an integral part of all ribosomes with the possible exception of some mitochondrial ribosomes (Borst & Grivell, 1971; Lizardi & Luck, 1971). Reconstitution experiments have clearly demonstrated the importance of prokaryotic 5S RNA for ribosomal function (Erdmann et al., 1971; Dohme & Nierhaus, 1976). It is generally accepted that 5S RNA plays a role in binding, directly or indirectly, some proteins to the large ribosomal subunit. In prokaryotes, 5S RNA is also thought to take part directly in protein synthesis by binding tRNA to the ribosome through base pairing (Erdmann, 1976). Some authors have speculated that cyclic conformational changes in prokaryotic 5S RNA may be the driving force for translocation in protein synthesis (Woese et al., 1975; Weidner et al., 1977).

Knowledge of the three-dimensional structure of 5S RNA derived by X-ray crystallography is, of course, an essential element in understanding its function. So far, studies used for probing the structure of 5S RNA in solution as well as in the ribosome have been limited to other techniques (Erdmann, 1976; Lewis & Doty, 1977; Österberg et al., 1976; Marshall & Smith, 1977; Wrede et al., 1978; Luoma & Marshall, 1978a,b; Chen et al., 1978; Hamill et al., 1978; Noller & Garrett, 1979). This has resulted in an abundance of models for the secondary structure of 5S RNA (Erdmann, 1976). Some studies suggest the existence of tertiary interactions within the 5S RNA molecule (Erdmann, 1976; Douthwaite et al., 1979; Noller & Garrett, 1979), but concrete information on this important aspect of the conformation is not yet available.

One important consideration in judging the feasibility of a proposed base-pairing scheme for prokaryotic 5S RNA ought to be the general applicability of the scheme. There is ample evidence from reconstitution experiments (Erdmann, 1976) that 5S RNA from one prokaryote can be incorporated into the large ribosomal subunit of another prokaryote without loss of biological activity. Therefore, the overall conformation of 5S RNA from various prokaryotes should be closely similar. The first model taking this fact fully into account is the one proposed by Fox & Woese (1975) which includes only those intramolecular double-helical regions that could be formed in all six prokaryotic 5S RNAs known at the time of its publication. Sequences of 5S RNA determined subsequently proved to conform to the model without fail. The model also is in good agreement with studies of the sites in the 5S RNA molecule sensitive to nuclease attack (Vigne & Jordan, 1971; Jordan, 1971; Bellemare et al., 1972a) or modifying agents (Lee & Ingram, 1969; Bellemare et al., 1972b; Gray et al., 1973; Noller & Herr, 1974; Delihas et al., 1975). It is, however, still at odds with other data pertaining to the secondary structure of prokaryotic 5S RNA, notably the oligonucleotide-binding studies of Wrede et al. (1978). More recent models, e.g., the model of Luoma & Marshall (1978b) and the model of Österberg et al. (1976), are also in good agreement with the nuclease-sensitive sites.

Secondary structure interactions between bases in an RNA chain can be studied with the aid of proton magnetic resonance. Although, as yet, it is not possible to deduce the conformation of an RNA molecule directly from the proton spectrum, the

† From the Department of Biophysical Chemistry, University of Nijmegen, Toernooiveld, 6525 ED Nijmegen, The Netherlands (P.J.M.S., A.H., and C.W.H), and the Department of Biochemistry, Free University, De Boelelaan 1083, 1081 HV Amsterdam, The Netherlands (H.A.R. and R.J.P.). *Received November 14, 1979.* This work was supported in part by the Netherlands Foundation for Chemical Research (SON) with financial aid from the Netherlands Organization for the Advancement of Pure Research (ZWO).

0006-2960/81/0420-0265$01.00/0

technique can be used to check proposed base-pairing schemes by comparing the experimentally obtained spectrum with that resulting from ring current shift calculations. This approach was used by Kearns & Wong (1974) in a proton NMR study on *Escherichia coli* 5S RNA. The resulting base-pairing model, however, is not generally applicable to prokaryotic 5S RNA (Raué et al., 1975).

In the present paper, the conformation of *Bacillus licheniformis* 5S RNA in solution is studied with the aid of ^1H and ^{31}P NMR. At 40 °C, the 360-MHz proton spectra, recorded in the spectral region between 14.5 and 10 ppm downfield from sodium 4,4-dimethyl-4-silapentanesulfonate (DSS), display a resolution approaching that obtained in low-field proton NMR spectra of tRNA. This resolution allows a comparison in some detail of the experimental spectrum to theoretical spectra derived from ring current shift calculations. The proton spectra also show resonances around 10.7 ppm most likely arising from hydrogen bonding of exocyclic amino protons in non-Watson–Crick base pairs involved in tertiary interactions (Reid et al., 1975; Steinmetz-Kayne et al., 1977; Geerdes, 1979) or from ring N protons of nonpaired bases which by the molecular folding are shielded from the solvent (Haasnoot et al., 1980). The resolved resonances observed in ^{31}P NMR spectra of *B. licheniformis* 5S RNA as well as those of *E. coli* 5S RNA point to the existence of special phosphodiester conformations in the sugar phosphate backbone of 5S RNA deviating from the g^-,g^- conformation found in A'RNA or A RNA double helices. The number of these special conformations in 5S RNA appears to be far smaller than in tRNA.

Materials and Methods

Isolation of 5S RNA. Late log phase *B. licheniformis* cells (strain S 244) grown on enriched nutrient broth (doubling time about 40 min) were resuspended in 1.5 volumes of 0.01 M Tris-HCl, pH 7.4, 0.01 M $MgCl_2$, 0.03 M NH_4Cl, 6 mM β-mercaptoethanol, and 0.1 mM dithiothreitol. The cells were lysed by incubation at 0 °C for 30 min with 1.0 mg/mL egg-white lysozyme (Sigma) followed by the addition of 0.1% (w/v) sodium deoxycholate. Viscosity was reduced by adding DNase (Sigma), and the suspension was passed once through a French press (Manton-Gaulin) at 9000 psi to complete breakage of the cells. Cell debris was removed by low-speed centrifugation, and ribosomes were isolated by the procedure of Fahnestock et al. (1974) in which the ribosomes are centrifuged through a dense layer of sucrose containing 0.5 M NH_4Cl. This effectively removes most of the adhering tRNA and an appreciable amount of extraneous protein from the ribosomes. Recentrifugation of the sucrose layer is, however, required to increase the yield of ribosomes.

The ribosomes were resuspended in TMK buffer (0.01 M Tris-HCl, pH 7.3, 0.01 M $MgCl_2$, and 0.05 M KCl), and RNA was extracted by the cold phenol–$NaDodSO_4$ method (Retêl & Planta, 1967). Subsequently, RNA was precipitated with ethanol and redissolved in TMK buffer. High molecular weight RNA was removed by adding solid NaCl to the RNA solution to a final concentration of 1.0 M. The precipitate was collected, dissolved in TMK buffer, and again salted out by addition of 1.0 M NaCl. The combined supernatants, containing high molecular weight RNA, 5S RNA, and tRNA in about equal amounts, were precipitated with ethanol, and the RNA was dissolved in a small volume of 0.01 M sodium acetate, pH 7.0, 0.01 M $MgCl_2$, 0.001 M EDTA, and 1.0 M NaCl. The 5S RNA was purified by two consecutive chromatographic runs on a Sephadex G-100 column (140 × 2.2 cm) using the same elution fluid. The 5S RNA was then precipitated with ethanol, dissolved in a small volume of distilled water, and desalted on a Sephadex G-25 column. Finally, the 5S RNA was lyophilized and its purity checked by Sephadex G-100 chromatography and polyacrylamide gel electrophoresis. The final preparation moved as a single symmetrical peak in both analyses, and its purity was judged to be better than 98%. The typical yield of 5S RNA was about 10 mg/100 g of cells.

Instrumentation. The ^{31}P NMR spectra were recorded on a Varian XL-100 spectrometer operating in the Fourier-transform mode at 40.5 MHz. Heteronuclear proton noise decoupling was used to remove the J coupling induced by the ribose protons. A pulse width of 20 μs was employed, corresponding to a flip angle of 45°. Accumulation proceeded during 16–20 h with a spectral width of 2000 Hz and an acquisition time of 1 s; no pulse delay was used. Usually, a sensitivity enhancement was applied, yielding a line broadening of 0.6 Hz. The spectra were recorded at 33 °C. The composition of the sample is described in the legends to the figures. Reported chemical shifts are given relative to 20% H_3PO_4 as an external reference with downfield shifts defined as positive. The D_2O solvent was used as an internal deuterium field-frequency lock.

High-resolution ^1H NMR spectra were obtained on a Bruker 360-MHz spectrometer operating in the correlation spectroscopy mode (Dadok & Sprecher, 1974; Gupta et al., 1974). A total of 1000 scans of 2 s each were accumulated in a Nicolet BNC-12 computer. Reported chemical shifts are given relative to sodium 4,4-dimethyl-4-silapentane-1-sulfonate (DSS), with downfield shifts defined as positive.

Ring current shift calculations for AU and GC base pairs were based on the ring current shift tables of Arter & Schmidt (1976), using intrinsic positions of 14.5 and 13.6 ppm, respectively. In several of the models for which spectra were simulated (see below), single noncomplementary residues are present. These are assumed to bulge out of the double helix without interrupting the RNA helix stacking (Lomant & Fresco, 1975). Stacking of single-strand residues at the end of double helices has not been taken into account, with the exception of A_{11}, which is assumed to be partly stacked upon the base pair G_{10}–C_{106} (see below). Resonance positions of GU base pairs were predicted on the basis of the ring current shift tables of Geerdes & Hilbers (1979), using intrinsic positions of 12.2 and 12.5 ppm for the GN_1H and UN_3H protons, respectively.

The number of hydrogen-bonded proton resonances in the 5S RNA spectrum between 14.5 and 12.0 ppm was determined by comparing the resonance intensity with that of a yeast $tRNA^{Phe}$ spectrum recorded under identical instrumental conditions which contains a known number of resonances (Robillard et al., 1977). The same number of scans was accumulated. The calibration was carried out at 35 °C. Alternatively the total resonance intensity of the 5S RNA spectra was determined by integration or simulation of the spectra taking either the resonance at 14.2 or 11.0 ppm as unity or the resonance at 14.0 ppm equal to two protons. Simulation of the spectra for this case and for the proposed secondary structure models (see above) was performed by summation of Lorentzian lines with a line width of 40 Hz.

Total magnesium concentrations were determined by atomic absorption spectrometry unless indicated otherwise.

Results

^1H NMR. A representative example of a hydrogen-bonded proton spectrum of *B. licheniformis* 5S RNA between 14.5 and 10.0 ppm, recorded at 40 °C, is presented in Figure 1. Under these conditions, well-resolved resonances can be dis-

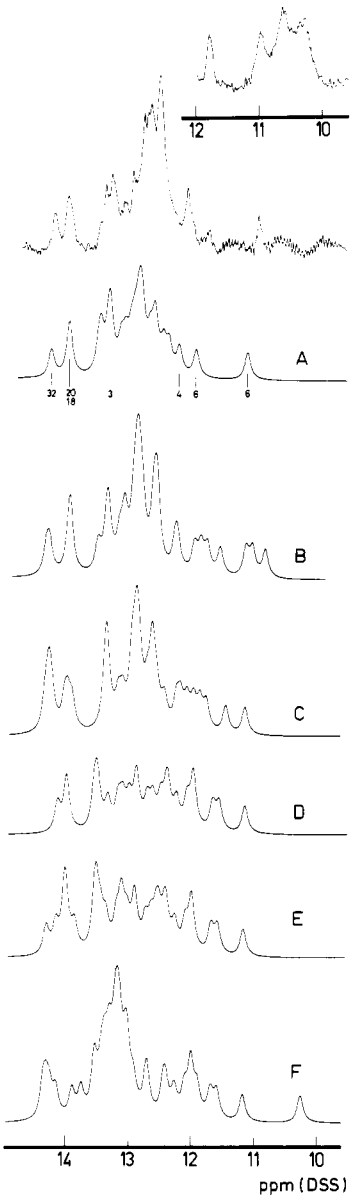

FIGURE 1: ^1H NMR spectrum (360 MHz) (top) of the hydrogen-bonded ring N protons of *B. licheniformis* 5S RNA. Solution conditions: 1 mM 5S RNA, 10 mM cacodylate, 10 mM EDTA, and estimated total Mg^{2+} concentration 8 mM, pH 7.0, in H_2O. The spectrum consists of 1000 accumulations recorded at 40 °C. The insert shows a section of the ^1H NMR spectrum, recorded at 29 °C; the vertical scale is expended by a factor of four. (A–F) Simulated spectra based on ring current calculations using the secondary structure according to (A) Fox & Woese (1975), (B) Österberg et al. (1976), (C) Luoma & Marshall (1978b), (D) Weidner et al. (1977), B model, (E) Kearns & Wong (1974), and (F) Cantor (1967). Because of their expected instability at 40 °C, the following base pairs have been omitted in the simulations: in (B) A_{71}–U_{101}, U_{72}–G_{100}, and C_{36}–G_{42}; in (C) G_{14}–U_{101}; C_{15}–G_{100}; in (F) G_{52}–U_{93} and U_{53}–G_{94}.

tinguished at 14.2, 14.0, 12.1, 11.8, and 11.0 ppm. The spectrum can be simulated by summing Lorentzian lines with a line width of 40 Hz. This is close to the value of 30 Hz used to simulate spectra of well-resolved tRNA's obtained under similar conditions (Reid et al., 1977). The number of resonances in the 5S RNA spectrum at 35 °C was determined by comparison to that of a yeast $tRNA^{Phe}$ spectrum, which under the conditions of the measurements contains 26 proton resonances between 14.5 and 11.5 ppm (Materials and Methods). This yielded 30 resonances between 14.5 and 12.0 ppm. For a number of other situations, the number of resonances was derived independently from simulated spectra (Materials and Methods). In this way, we find 31 resonances between 14.5 and 12.0 ppm at 29 °C. In addition, two resonances from a GU pair (at 11.8 and 11.0 ppm) and another four resonances around 10.7 ppm are present at this temperature (see Figure 1, insert). At 40 °C this procedure yields 27 resonances between 14.5 and 12.0 ppm. Therefore these integrations indicate that between 14.5 and 12.0 ppm the spectral intensity increases by about three to four resonances when the temperature is lowered from 40 to 29 °C. At 29 °C the resolution of the spectrum is somewhat less than that at 40 °C. This may be due to the increased number of resonances, giving rise to increased overlap, and also to an increase of the rotational correlation time of the molecules.

Various models have been proposed for the secondary structure of prokaryotic 5S RNA (Erdmann, 1976). In Figure 2 the secondary structure 5S RNA according to some current models of *B. licheniformis* is presented.

The Fox and Woese model (Figure 2A) was the first to be universally applicable; i.e., it includes those intramolecular double-helical regions which can be formed in all prokaryotic 5S RNAs sequenced to date. Several of its double-helical regions, notably the molecular stalk and the prokaryotic loop, are common features in the other models (see Figure 2), and we will refer frequently to these helices below.

For each of these models, the distribution of the resonances of the hydrogen-bonded protons was determined by calculating ring current shifts exerted by neighboring bases. The resulting spectra are shown in Figure 1A–F.

Spectral Region from 14.5 to 13.5 ppm. The experimental spectrum displays a single well-resolved resonance at 14.2 ppm and two resonances super-imposed upon each other at 14.0 ppm. As can be seen from Figure 1, for all models three or more resonances are predicted in this region. For the Fox and Woese model, these are the hydrogen-bonded resonances from the base pairs A_{18}–U_{61}, A_{20}–U_{59}, and A_{46}–U_{32} (see Figure 1A). Base pair A_{114}–U_2 present in the molecular stalk of all models in Figure 2 is also predicted in this spectral region, i.e., at 13.8 ppm. However, because the helix in question ends with a weak GU interaction and because fraying effects are often seen at the ends of double helices, we do not expect this AU pair to contribute to the low-field ^1H spectrum (Baan et al., 1977). Therefore, in all simulated spectra, a resonance from this base pair is not incorporated.

Spectral Region from 13.5 to 12.0 ppm. In this region most of the resonances are crowded together, giving rise to strongly overlapping lines from which the resonances around 13.3 and at 12.1 ppm stand out. Among other base pairs, A_{113}–U_3 from the molecular stalk is predicted to contribute to the resonance intensity at 13.3 ppm. At 12.1 ppm, the spectrum shows a single peak consisting of two superimposed ^1H resonances. Ring current calculations place the resonance of the G_4–G_{112} pair from the molecular stalk at this position (Figure 1).

Spectral Region from 12.0 to 10.0 ppm. At 29 °C (Figure 1, insert), five resonances are observed between 11 and 10 ppm. Because of their position, these resonances cannot arise from normal Watson–Crick base pairs. In analogy with the results obtained for tRNAs, they can be attributed to ring N protons involved in hydrogen bonding to carbonyl groups, as, for instance, in GU base pairs, and to exocyclic amino protons involved in hydrogen bonding of other non-Watson–Crick base pairs. The latter type of proton resonances is indicative of the presence of tertiary structure in the molecule (Reid et al., 1975; Steinmetz-Kayne et al., 1977; Geerdes, 1979). It is noted that some of these resonances may also arise from U's or G's not involved in base pairing (Haasnoot et al., 1980). Most of these resonances are melted out at 40 °C (Figure 1). The resonance

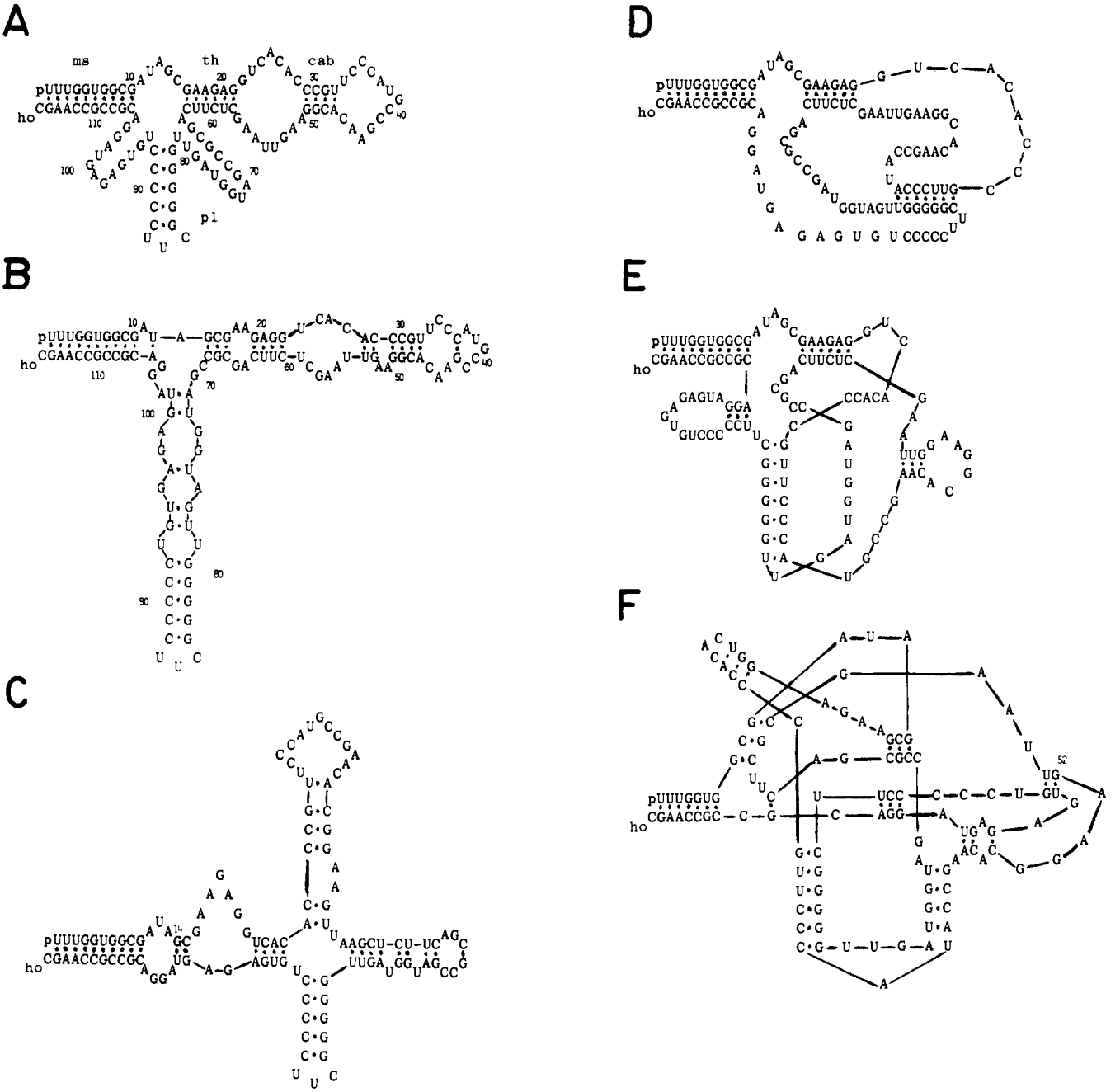

FIGURE 2: Secondary structures of *B. licheniformis* 5S RNA according to the models proposed by (A) Fox & Woese (1975), (B) Österberg et al. (1976), (C) Luoma & Marshall (1978b), (D) Weidner et al. (1977) B model, (E) Kearns & Wong (1974), and (F) Cantor, 1967. Abbreviations used in (A): ms, molecular stalk; th, tuned helix; cab, common arm base; pl, prokaryotic loop. In the original B model of Weidner et al. (1977), the double helix equivalent to the tuned helix has been left out.

at 11.0 ppm, which is not melted out at 40 °C, is assigned to a more stable GU pair internal in a double-helical stack. The argument for this assignment is discussed below. In the Fox and Woese model of *B. licheniformis* 5S RNA, the G_{110}–U_6 base pair internal in the molecular stalk (Figure 2A) forms the only possible candidate for this resonance. As mentioned before, the G_{115}–U_1 pair at the terminus of the molecular stalk is not expected to contribute to the proton spectrum due to fraying effects. In contrast to GC and AU pairs, a GU base pair contributes two resonances to the low-field NMR spectrum, i.e., a GN_1H and a UN_3H proton resonance (Baan et al., 1977; Johnston & Redfield, 1978). The resonance positions of these two protons in the G_{110}–U_6 base pair were estimated by calculating the ring current shifts induced by nearest and next-nearest bases. Using the ring current shift table (Geerdes & Hilbers, 1979), we obtained positions of 11.2 and 12.0 ppm for the GN_1H and the UN_3H proton, respectively. This is close to the experimentally observed positions at 11.0 and 11.8 ppm.

Temperature Dependence of the Low-Field ^1H NMR Spectra. As has been mentioned, increasing the temperature from 29 to 40 °C seems to result in a disappearance of a few resonances between 14.5 and 12.0 ppm in addition to the loss of resonances around 10.7 ppm. The melting of the molecule can be followed in much more detail above 40 °C. In figure 3, NMR spectra recorded at various temperatures between 40 and 53 °C have been collected. In this series of experiments, the Mg^{2+} concentration was higher than that in Figure 1. As a result, resonance intensity is still visible at 40 °C around 10.7 ppm; it disappears at 48 °C (Figure 3). Between 14.5 and 12.0 ppm, some resonances are seen to be slightly shifted when the experimental 40 °C spectra in Figures 1 and 3 are compared. However, the total number of proton resonances in this spectral region remains constant within the limits of experimental accuracy.

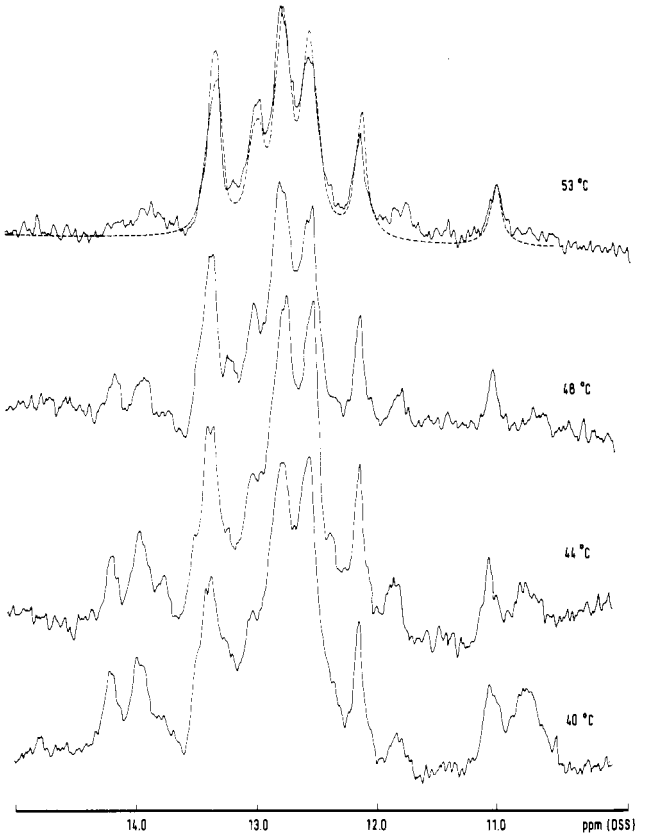

FIGURE 3: ^{1}H NMR spectra (360 MHz) of the hydrogen-bonded ring N protons of *B. licheniformis* 5S RNA recorded as a function of temperature between 40 and 53 °C. Solution conditions: 1 mM 5S RNA, 10 mM cacodylate, 10 mM EDTA, and total Mg^{2+} concentration 15 mM, pH 7.0, in H_2O. The spectra consist of 1000 accumulations each. The dashed line in the 53 °C spectrum represents the simulated spectrum (see text).

The melting process above 40 °C has been followed by simulating the spectra, taking the resonance at 11.0 ppm as unity (see Materials and Methods). This was most easily achieved by starting with the spectrum recorded at 53 °C, which has the best resolution. This spectrum could be simulated by summing 16 Lorentzian lines, omitting the residual resonance at 11.8 ppm (dashed line in the 53 °C spectrum of Figure 3). Subsequently, all other spectra in Figure 3 and Figure 4A could be simulated by adding or subtracting resonances; occasionally a small shift of a few hundredths of a parts per million had to be introduced. It follows from these simulations that upon raising the temperature from 40 to 53 °C a total of about 12 resonances is lost between 14.5 and 12.0 ppm, three of which are the AU resonances at 14.2 and 14.0 ppm. At 48 °C, the latter resonances have hardly broadened but rather have diminished in intensity. This means that they disappear in an equilibrium process in which the double helix population of these AU pairs decreases. In this case, the dissociation rate constant of the double helix concerned will be less than 10^2 s^{-1} (Crothers et al., 1973). The melting of the AU resonances follows closely upon the loss of the resonances around 10.7 ppm which are the first to disappear when the temperature is raised (Figure 3). It is therefore interesting to note that at 53 °C the resonance at 11.0 ppm is still visible in the spectrum. Apparently its melting not only is decoupled from the "melting" of the tertiary structure, as witnessed by the earlier melting of the resonances around 10.7 ppm, but also from the melting of part of the secondary structure since about 12 resonances between 14.5 and 12.0 ppm have disappeared from the spectrum at 53 °C. It is for this reason that we have assigned the resonance at 11.0 ppm to a GU pair in

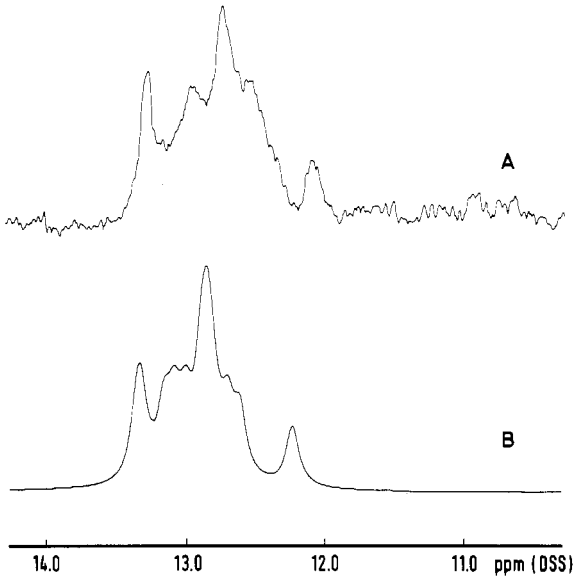

FIGURE 4: (A) ^{1}H NMR spectrum (360 MHz) of the hydrogen-bonded ring N protons of *B. licheniformis* 5S RNA recorded at 57 °C. Solution conditions are the same as those of Figure 3. The spectrum consists of 1000 accumulations. (B) Simulated spectrum of the molecular stalk and the prokaryotic loop based on ring current calculations.

an internal position in a double-helical stack. The resonance at 11.8 ppm which was also attributed to this base pair broadens somewhat before the resonance at 11.0 ppm, but both resonances disappear in the narrow temperature range between 53 °C and 57 °C (compare Figure 3 and Figure 4A). A similar melting behavior of a GU pair has been observed before (Baan et al., 1977).

The spectrum at 57 °C consists of 13 resonances. The most likely contributors to this spectrum are the molecular stalk and the prokaryotic loop. Among the possible double helices which on the basis of a base-pairing matrix can be formed in *B. licheniformis* 5S RNA, these two are the most stable. When the thermodynamic parameters of Gralla & Crothers (1973), Borer et al. (1974), and Tinoco et al. (1971) are used, melting temperatures of 82 and 92 °C are predicted for the molecular stalk and prokaryotic loop, respectively. For the prokaryotic loop, we choose the most stable form with four GC pairs in the stem and five bases in the loop. The ΔG for formation of the latter hairpin is calculated to be −3.6 kcal/mol at 57 °C. For the molecular stalk, we calculate the ΔG for hairpin formation to be equal to −6.6 kcal/mol at 57 °C. Therefore we expect that the resonances of these two double helices will still be visible at 57 °C. The overlap of the resonances in the 57 °C spectrum hampers its use as a definitive test of the base-paired sequences really present in solution. However, the intensities at 13.2, 12.6, and 12.1 ppm may serve as indications for the "integrity" of the prokaryotic loop and the molecular stalk. Empirical resonance positions of base pairs, sandwiched between certain other base pairs, are available from model system studies (C.W. Hilbers, unpublished results). This way we find G_4–C_{112} at 12.0 ppm. None of the other base pairs is found to resonate at that position. Furthermore, on this basis, the three base pairs G_{81}–C_{91}, G_{82}–C_{90}, and G_{83}–C_{89} in the prokaryotic loop are predicted to resonate at 12.7 ppm. Finally, the base pairs C_5–C_{111} and G_8–C_{108} will give rise to resonances at 13.2 and 13.1 ppm. In addition, ring current calculations have been performed to predict the spectrum of the molecular stalk and the prokaryotic loop. The simulated spectrum is given in Figure 4B. It was assumed that A_{11} is partly stacked upon G_{10}–C_{106}, yielding an extra upfield shift

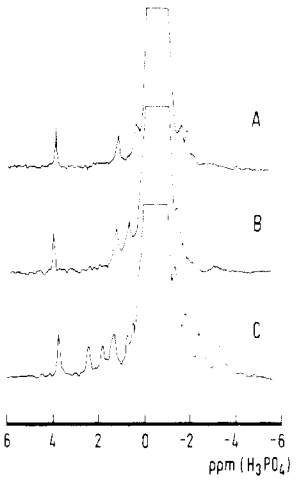

FIGURE 5: ^{31}P NMR spectra (40.5 MHz) of *B. licheniformis* 5S RNA (A), *E. coli* 5S RNA (B), and yeast tRNA^{Phe} (C) recorded at 33 °C. The main resonance in each of the spectra has been cut off at about the half-height. Solution conditions for both 5S RNA samples: 1 mM 5S RNA, 30 mM cacodylate, 80 mM NaCl, 1 mM EDTA, and estimated total Mg^{2+} concentration 8 mM, pH 7.5, in D_2O. Solution conditions for tRNA sample: 1 mM tRNA, 80 mM NaCl, 30 mM cacodylate, 10 mM $MgCl_2$, and 1 mM EDTA, pH 7.0, in D_2O.

of 0.3 ppm of the corresponding resonance. As has been discussed, A_{114}–U_2 and G_{115}–U_1 are not expected to contribute to the spectrum and have not been incorporated. This is also the case for G_{110}–U_6, the resonances of which have been omitted as well. The similarity of the experimental and the theoretical spectrum is remarkable. In view of the limitations of this type of calculations, we consider this as somewhat fortuitous. However, combining these results, i.e., the expected stability of the helices, the number of resonances in the spectrum, and the positions of the marker resonances and those expected for particular base pairs in the helices as well as the agreement between the calculated and experimental spectrum, there is a reasonable basis for assuming that the molecular stalk and the prokaryotic loop are indeed present in solution at 57 °C. When measurements were performed at temperatures higher than 60 °C, the spectra subsequently obtained at lower temperatures were not reproducible. This may be the result of hydrolysis due to the Mg^{2+} concentrations present in the samples (Weidner et al., 1977). No such effects were observed at 57 °C. When 5S RNA was kept at this temperature for several hours and then cooled, spectra recorded at 40 °C were virtually equivalent to those obtained prior to heating.

^{31}P NMR. The proton NMR experiments described in the preceding section have been supplemented by ^{31}P NMR experiments. In Figure 5, ^{31}P spectra of 5S RNA of *B. licheniformis* (Figure 5A) as well as of *E. coli* (Figure 5B), recorded at 33 °C, are compared with a ^{31}P spectrum of yeast tRNA^{Phe} (Figure 5C) obtained under similar solution conditions.

The spectra are characterized by one large resonance (cut off at about half-height) around 0 ppm coming from the majority of the diester phosphates in these RNA species. At both sides of the main resonance, resolved resonances are visible. For all three RNAs, the low-field resonances close to 3.5 ppm can be assigned to the 5′-terminal monoester phosphate on the basis of their pH dependence (Guéron & Shulman, 1975). It has been shown earlier (Salemink et al., 1979) that about 17 diester phosphates in yeast tRNA^{Phe} are contributing to the resolved resonances in its ^{31}P NMR spectrum (Figure 5C). Integration of the spectra in Figure 5A,B shows that in 5S RNA only four diester phosphate groups give rise to such resolved resonances. We have demonstrated that the resolved resonances in the spectrum of yeast tRNA^{Phe} are due either to diester phosphates having conformations differing from the g^-,g^- conformation or to diester phosphates involved in hydrogen bonds (Salemink et al., 1979). These special conformations are imposed by the tertiary structure or by the interactions within the loops. Therefore we conclude that in the three-dimensional structure of 5S RNA, under our experimental conditions, only four diester phosphates, deviating from the g^-,g^- conformation and/or involved in hydrogen bonding, are present. Apparently the phosphate backbone in 5S RNA is much less constrained by the tertiary structure than that of tRNA.

A comparison of the ^{31}P spectra of the two prokaryotic 5S RNA species (Figure 5A,B) shows that they are not quite identical. This may reflect different values of the torsional angles ω,ω' and/or the bond angle θ of the respective phosphate groups.

Discussion

Hydrogen Bonding in B. licheniformis 5S RNA. One of the important questions to be answered in a structure determination of 5S RNA concerns the number of base pairs present in the molecule. We have approached this problem by comparing the low-field ^{1}H NMR spectrum of yeast tRNA^{Phe}, which contains a known number of hydrogen-bonded ring N proton resonances, with that of 5S RNA of *B. licheniformis*. From this comparison it follows that below 40 °C the 5S RNA spectrum contains close to 30 hydrogen-bonded ring N resonances between 14.5 and 12.0 ppm downfield from DSS. The same result is obtained when experimental and simulated spectra are compared. Because of fraying effects, resonances from some base pairs may be absent from the spectra, even though the base pairs are intact during 90% of the time. The base pair A_{114}–U_2 (Figure 2) is likely to be susceptible to such fraying. Therefore the number of base pairs calculated above is a lower limit. In addition, two resonances have been assigned to a GU base pair, while four resonances around 10.7 ppm have been attributed to protons involved in non-Watson–Crick base-pair formation. This brings the total number of base pairs present in 5S RNA from B. licheniformis below 40 °C to at least 35. Our estimate of the absolute number of resonances in the spectra is necessarily rather inaccurate; e.g., in order to compare 5S RNA and tRNA spectra, the sample tubes have to be interchanged. We estimate the accuracy to be ±5 proton resonances. The relative intensity of the various resonances in a particular spectrum can be determined reasonably well by simulation. When a particular proton resonance is used as a standard, the accuracy in determining the total intensity within a single spectrum is estimated to be ±2 proton resonances. Kearns & Wong (1974) have also estimated the number of base pairs in 5S RNA from *E. coli* by comparing its spectrum to that of yeast tRNA^{Phe}. At the time of publication of their estimate, the number of hydrogen-bonded resonances for yeast tRNA^{Phe} was taken to be 19. When the presently accepted value of 26 resonances is used (Robillard et al., 1977), we arrive at an estimate of 36 resonances in *E. coli* 5S RNA between 14.5 and 11.0 ppm at 30 °C. Taking into account the difference in experimental conditions, this is close to the number obtained in our experiments. Most other techniques used in determining the extent of base pairing in 5S RNA yield values close to or higher than 36 (Erdmann, 1976). An exceptionally high estimate was obtained recently from an infrared study of *B. stearothermophilus* and *E. coli* 5S RNA. This study indicated a number of 46 and 56 base pairs for the two 5S RNA species,

Table I: Common Features in the Secondary Structure of Various Models Proposed for 5S RNA

double helix[b]	model[a] F&W	K&W	L&M	Ö	W	C
ms	+	+	+	+	+	(±)[c]
th	+	+	−	−	(−)[d]	−
cab	+	−	+	+	−	−
pl	+	−	+	+	−	−

[a] The various models are the following: F&W Fox & Woese (1975); K&W, Kearns & Wong (1974); L&M, Luoma & Marshall (1978b); Ö, Osterbert et al. (1976); W, Weidner et al. (1977); C, Cantor (1967). [b] Abbreviations used: ms, molecular stalk; th, tuned helix; cab, common arm base; pl, prokaryotic loop. [c] The cantor model comprises only the first seven base pairs of the molecular stalk. [d] Although the formation of a double helix equivalent to the tuned helix in principle is possible, Weidner et al. (1977) have deliberately left out this helix.

respectively, at 20 °C (Appel et al., 1979). All these studies converge on the conclusion that the number of base pairs present in the 5S RNA structure is larger than that derived from the Fox & Woese (1975) model. More in particular, our results for *B. licheniformis* 5S RNA demonstrate that the 23 Watson–Crick base pairs present in the Fox and Woese model of this RNA are insufficient to explain all resonances observed in the proton NMR spectrum below 40 °C. Of course, the model, which is exclusively a secondary structure model, does not account for the tertiary resonances. Neither, for that matter, does any of the other secondary structure models proposed. Despite the discrepancy between the number of resonances observed in the ^{1}H NMR spectra and the number of base pairs present in the Fox and Woese model, our data support the presence of several elements of the model in the conformation of 5S RNA. The existence of the molecular stalk is strongly supported by the GU resonances at positions close to those predicted for G_{110}–U_6 and by the marker resonances in the 57 °C spectrum. The disappearance of the GU resonances at 57 °C does not imply that the molecular stalk is not intact at 57 °C. The reason is that GU base pairs positioned internally in a helical stack can open up at a faster rate than the helix itself (Rhodes, 1977; Johnston & Redfield, 1978). The high-temperature spectra obtained in the NMR study of *E. coli* 5S RNA by Kearns & Wong (1974) are also in agreement with the presence of a molecular stalk in this molecule. Evidence for the existence of both the molecular stalk and the prokaryotic loop is also provided by experiments on the RNase sensitivity of 5S RNA. Douthwaite et al. (1979) showed that in *E. coli* 5S RNA both regions are resistant to low concentrations of RNase A and RNase T_2. The G residues from the prokaryotic loop of *B. licheniformis* 5S RNA are completely resistant to low concentrations of RNase T_1 even at 50 °C in 7 M urea (W. J. Stiekema and H. A. Raué, unpublished results). Moreover, the prokaryotic loop can be isolated as such from partial RNase T_1 digests of *B. licheniformis* 5S RNA (Raué et al., 1975). The existence of the molecular stalk and prokaryotic loop, therefore, appears now to be well documented.

It seems likely, in view of the combined evidence for the existence of the prokaryotic loop discussed above, that the models that do not incorporate this feature can be discarded. This includes the models of Kearns & Wong (1974) and Cantor (1967) and the B model of Weidner et al. (1977) (see Figure 2 and Table I). The remaining models, i.e., the model of Fox & Woese (1975), of Österberg et al. (1976), and of Luoma & Marshall (1978b), give rise to three or more AU resonances between 14.5 and 13.5 ppm. In the Fox and Woese model, three AU pairs from the tuned helix and the common arm base are responsible for these resonances. Since the experimental spectrum at 40 °C displays three proton resonances in this region, our NMR data are certainly not inconsistent with the occurrence of these two structural elements. The other two models have the common arm base, which provides one resonance to this spectral region, in common with the Fox and Woese model. The other AU resonances are coming from other structural elements in these models. As mentioned above, an important shortcoming of the Fox and Woese model is its low number of base pairs. When comparing the experimental spectrum (top spectrum, Figure 1) with the simulated spectrum (Figure 1A), it appears that especially around 12.6 ppm intensity is missing in the simulated spectrum. In this respect, it seems noteworthy that the secondary structure of *B. licheniformis* 5S RNA, as described by Fox and Woese's model, can be extended by some additional GC base pairs, namely, G_{65}–C_{15}, G_{14}–C_{66}, G_{104}–C_{68}, and G_{103}–C_{69}, which would provide extra resonance intensity in this spectral region. These base-pairing possibilities are highly conserved in prokaryotic 5S RNA (Erdmann, 1980). The models of Österberg et al. (1976) and of Luoma & Marshall (1978a,b) have a higher number in base pairs and as a result have more resonance intensity around 12.6 ppm in their simulated spectra (see Figure 1). On the other hand, these simulated spectra display too much intensity between 14.5 and 13.5 ppm and between 12 and 11 ppm with respect to the experimental spectrum. At this moment, the available experimental data as well as the uncertainties inherent in the simulations do not permit us to discriminate between the presence or absence of certain elements which in these models are different, e.g., the tuned helix in the Fox and Woese model vs. the base-paired region of residues 14–22 in the model of Österberg et al. (1976).

Folding of the Molecule. From the ^{31}P spectra (Figure 5), it is concluded that the number of special conformations in the sugar phosphate backbone of 5S RNA is much less than in tRNA. In tRNA, these special conformations arise because the molecule is folded into a compact structure in which the TΨC loop and the DHU loop, which are far apart in the secondary structure, interact. As a result, several phosphate groups are forced out of their normal lowest energy state, i.e., the g^-,g^- conformation with respect to torsional angles ω' and ω. Apparently such compact folding patterns are less pronounced in 5S RNA. The model inferred from small-angle X-ray scattering experiments in which 5S RNA is considerably more elongated than tRNA (Österberg et al., 1976) may form the explanation for our ^{31}P NMR observations. Moreover, the elongated conformation of the 5S RNA molecule, in which there would be little interaction between the various double-helical segments, may also explain the sequential melting of the molecule observed in the ^{1}H NMR spectra of Figures 3 and 4A. This sequential process is observed in the presence of Mg^{2+} ions (Figure 3). The first part to melt out is the tertiary structure, followed by secondary structural elements. The disruption of the tertiary structure clearly depends on the Mg^{2+} concentration (see Results). Under our solution conditions, its T_m does not appear to be sufficiently raised so as to couple to the rest of the melting transitions. This is contrary to experience with tRNA (Römer & Hach, 1975; Stein & Crothers, 1976). It may be a general property of 5S RNA structure since also for *E. coli* 5S RNA sequential melting has been observed in the presence of Mg^{2+} (Kearns & Wong, 1974). The disruption of the 5S RNA tertiary structure proceeds at physiological temperature. It, therefore, may

reflect possible rearrangements of the 5S RNA conformation during protein biosynthesis (Woese et al., 1975; Weidner et al., 1977).

Acknowledgments

We gratefully acknowledge the Netherlands Organization for the Advancement of Pure Research (Z.W.O.) for support of the 360-MHz NMR facility at Groningen, K. Dijkstra and Dr. R. Kaptein for keeping the apparatus in excellent condition, and J. van Kessel for technical assistance. Finally, we thank Dr. V. Erdmann for making available his infrared results prior to publication and M. M. C. Duin for expert assistance in preparing various samples.

References

Appel, B., Erdmann, V. A., Stultz, J., & Ackermann, Th. (1979) *Nucleic Acids Res. 7*, 1043.

Arter, D. B., & Schmidt, P. G. (1976) *Nucleic Acids Res. 3*, 1437.

Baan, R. A., Hilbers, C. W., Van Charldorp, R., Van Leerdam, E., Van Knippenberg, P. H., & Bosch, L. (1977) *Proc. Natl. Acad. Sci. U.S.A. 74*, 1028.

Bellemare, G., Jordan, B. R., & Monier, R. (1972a) *J. Mol. Biol. 71*, 307.

Bellemare, G., Jordan, B. R., Rocca-Sera, J., & Monier, R. (1972b) *Biochimie 54*, 1453.

Borer, P. N., Dengler, B., Tinoco, I., & Uhlenbeck, O. C. (1974) *J. Mol. Biol. 86*, 843.

Borst, P., & Grivell, L. A. (1971) *FEBS Lett. 13*, 73.

Cantor, C. R. (1967) *Nature (London) 216*, 513.

Chen, M. C., Geigé, R., Lord, R. C., & Rich, A. (1978) *Biochemistry 17*, 3134.

Crothers, D. M., Hilbers, C. W., & Shulman, R. G. (1973) *Proc. Natl. Acad. Sci. U.S.A. 70*, 2899.

Dadok, J., & Sprecher, R. (1974) *J. Magn. Reson. 13*, 243.

Delihas, N., Dunn, J. J., & Erdmann, V. A. (1975) *FEBS Lett. 58*, 76.

Dohme, F., & Nierhaus, K. N. (1976) *Proc. Natl. Acad. Sci. U.S.A. 73*, 2221.

Douthwaite, S., Garrett, R. A., Wagner, R., & Feunteun, J. (1979) *Nucleic Acids Res. 6*, 2453.

Erdmann, V. A. (1976) *Prog. Nucleic Acid Res. Mol. Biol. 18*, 45.

Erdmann, V. A. (1980) *Nucleic Acids Res. 8*, 31.

Erdmann, V. A., Fahnestock, S., Higo, K., & Nomura, M. (1971) *Proc. Natl. Acad. Sci. U.S.A. 68*, 2932.

Fahnestock, S., Erdmann, V. A., & Nomura, M. (1974) *Methods Enzymol. 30*, 554.

Fox, G. E., & Woese, C. R. (1975) *Nature (London) 256*, 505.

Geerdes, H. A. M. (1979) Thesis, University of Nijmegen.

Geerdes, H. A. M., & Hilbers, C. W. (1979) *FEBS Lett. 107*, 125.

Gralla, J., & Crothers, D. M. (1973) *J. Mol. Biol. 73*, 497.

Gray, P. N., Bellemare, G., Monier, R., Garrett, R. A., & Stöffler, G. (1973) *J. Mol. Biol. 77*, 133.

Guéron, M., & Shulman, R. G. (1975) *Proc. Natl. Acad. Sci. U.S.A. 72*, 3482.

Gupta, R., Ferretti, J., & Becker, E. D. (1974) *J. Magn. Reson. 13*, 275.

Haasnoot, C. A. G., Den Hartog, J. H. J., De Rooy, F. M., Van Boom, J. H., & Altona, C. (1980) *Nucleic Acids Res. 8*, 169.

Hamill, W. D., Jr., Grant, D. M., Cooper, R. B., & Harmon, S. A. (1978) *J. Am. Chem. Soc. 100*, 633.

Johnston, P. D., & Redfield, A. G. (1978) *Nucleic Acids Res. 5*, 3913.

Jordan, B. R. (1971) *J. Mol. Biol. 55*, 423.

Kearns, D. R., & Wong, Y. P. (1974) *J. Mol. Biol. 87*, 755.

Lee, J. C., & Ingram, V. M. (1969) *J. Mol. Biol. 41*, 431.

Lewis, J. B., & Doty, P. (1977) *Biochemistry 16*, 5016.

Lizardi, P. M., & Luck, D. J. L. (1971) *Nature (London), New Biol. 229*, 140.

Lomant, A. J., & Fresco, J. R. (1975) *Prog. Nucleic Acid Res. Mol. Biol. 15*, 185.

Luoma, G. A., & Marshall, A. G. (1978a) *J. Mol. Biol. 125*, 95.

Luoma, G. A., & Marshall, A. G. (1978b) *Proc. Natl. Acad. Sci. U.S.A. 75*, 4901.

Marshall, A. G., & Smith, J. L. (1977) *J. Am. Chem. Soc. 99*, 635.

Noller, H. F., & Herr, W. (1974) *J. Mol. Biol. 90*, 181.

Noller, H. F., & Garrett, R. A. (1979) *J. Mol. Biol. 132*, 621.

Österberg, R., Sjöberg, B., & Garrett, R. A. (1976) *Eur. J. Biochem. 68*, 481.

Rauê, H. A., Stoof, T. J., & Planta, R. J. (1975) *Eur. J. Biochem. 59*, 35.

Reid, B. R., Ribeiro, N., Gould, G., Robillard, G. T., Hilbers, C. W., & Shulman, R. G. (1975) *Proc. Natl. Acad. Sci. U.S.A. 72*, 2049.

Reid, B. R., Ribeiro, S., McCollum, L., Abbate, J., & Hurd, R. E. (1977) *Biochemistry 16*, 2086.

Retèl, J., & Planta, R. J. (1967) *Eur. J. Biochem. 3*, 248.

Rhodes, D. (1977) *Eur. J. Biochem. 81*, 91.

Robillard, G. T., Tarr, C. E., Vosman, F., & Reid, B. R. (1977) *Biochemistry 16*, 5261.

Römer, R., & Hach, R. (1975) *Eur. J. Biochem. 55*, 271.

Salemink, P. J. M., Swarthof, T., & Hilbers, C. W. (1979) *Biochemistry 18*, 3477.

Stein, A., & Crothers, D. M. (1976) *Biochemistry 15*, 160.

Steinmetz-Kayne, M., Benigno, R., & Kallenbach, N. R. (1977) *Biochemistry 16*, 2064.

Tinoco, I., Uhlenbeck, O. C., & Levine, M. D. (1971) *Nature (London) 230*, 362.

Vigne, R., & Jordan, B. R. (1971) *Biochimie 53*, 981.

Weidner, H., Yuan, R., & Crothers, D. M. (1977) *Nature (London) 266*, 193.

Woese, C. R., Pribula, C. D., Fox, G. E., & Zablen, L. B. (1975) *J. Mol. Evol. 5*, 35.

Wrede, P., Pongs, O., & Erdmann, V. A. (1978) *J. Mol. Biol. 120*, 83.